Ligand-Dependent Tau Filament Formation: Implications for Alzheimer's Disease Progression†

Michelle E. King,‡ Vibha Ahuja,‡ Lester I. Binder,‡ and Jeff Kuret*,§

Department of Cell and Molecular Biology, Northwestern University Medical School, Chicago, Illinois 60611, and Department of Medical Biochemistry, The Ohio State University College of Medicine, Columbus, Ohio 43210

Received May 21, 1999; Revised Manuscript Received September 8, 1999

ABSTRACT: The mechanism through which arachidonic acid induces the polymerization of tau protein into filaments under reducing conditions was characterized through a combination of fluorescence spectroscopy and electron microscopy. Results show that polymerization follows a ligand-mediated mechanism, where binding of arachidonic acid is an obligate step preceding tau−tau interaction. Homopolymerization begins with rapid (on the order of seconds) nucleation, followed by a slower elongation phase (on the order of hours). Although essentially all synthetic filaments have straight morphology at early time points, they interact with thioflavin-S and monoclonal antibody Alz50 much like authentic paired helical filaments, suggesting that the conformation of tau protein is similar in the two filament forms. Over a period of days, synthetic straight filaments gradually adopt paired helical morphology. These results define a novel pathway of tau filament formation under reducing conditions, where oxidation may contribute to final paired helical morphology, but is not a necessary prerequisite for efficient nucleation or elongation of tau filaments.

Evidence suggests that the polymerization of tau into filaments plays a decisive role in the chain of events that culminate in neuronal death (*1*). The phenomenon is not unique to AD,[1] but common to a wide range of neurodegenerative disorders, including *dementia pugilistica*, postencephalitic parkinsonism, adult Down Syndrome, Pick's disease, and myotonic dystrophy (*2*). Although tau filaments appear in a stereotypic manner during progression of these diseases, the temporal and spatial distribution of neurons that develop the pathology is disease-dependent (*3, 4*). In fact, the development of neurofibrillary pathology may represent part of a final common pathway of neurodegeneration that is initiated in response to diverse insults in different brain regions.

Tau filaments appear in two morphologies: SFs, which average 10−15 nm in width; and PHFs, which are up to 20 nm in width and have a helical pitch associated with them. The two forms are closely related structurally, copurify with one another, and share epitopes recognized by monclonal antibodies (*5, 6*). Although it has been argued that SFs are precursors of PHFs in AD (*7*), the forces that give rise to either morphology are unknown. Tau protein does not polymerize spontaneously at physiological concentrations (low micromolar), and efforts to stimulate the polymerization of recombinant tau by changing its state of phosphorylation alone have failed.

These data suggest that an additional factor is required to guide the formation of tau filaments. Indeed, it has been shown that a variety of anionic species can promote tau polymerization, guiding the formation of SFs and PHFs from recombinant tau (*8*−*11*). Two principal pathways have been proposed: oxidation dependent and oxidation independent. The former pathway requires covalent disulfide bond formation between tau protomers before assembly is mediated by polyanions such as heparin or RNA (*11, 12*). Proteolytic fragments containing the C-terminal third of tau assemble better than intact tau under these conditions (*12, 13*). The oxidation-independent pathway proceeds under reducing conditions from full-length tau monomer, and does not require proteolysis for efficient rates of reaction (*14*).

Recently we showed that fatty acids are extremely powerful inducers of tau polymerization under near-physiological conditions of pH, salt concentration, temperature, and reducing environment (*14*). Here we employ these agents to assess the mechanism of tau polymerization by the oxidation-independent pathway. The results show how filament formation can begin in normal neurons before major changes in the redox state of the cell have occurred.

EXPERIMENTAL PROCEDURES

Materials. Full-length monomeric recombinant tau protein (htau40) and monoclonal antibodies Alz50 (*15*) and Tau5 (*16*) were purified and handled as described (*17*). AA was from Fluka (Ronkonkoma, NY), whereas DTT and ThS were from Sigma (St. Louis, MO). PHF was purified as described previously (*18*) and supplied by Dr. Hanna Ksiezak-Reding

† Supported by grants from the NIH (AG14452; AG14453) and the Alzheimer's Association (RG2-29-076).

* To whom correspondence should be addressed at the Department of Medical Biochemistry, The Ohio State University College of Medicine, Columbus, OH 43210. Telephone: (614) 688-5899. FAX: (614) 292-5379. Email: kuret.3@osu.edu.

‡ Northwestern University Medical School.

§ The Ohio State University College of Medicine.

[1] Abbreviations: AA, arachidonic acid; AD, Alzheimer's disease; DTT, dithiothreitol; PHF, paired helical filament; SF, straight filament; ThS,thioflavin-S.

10.1021/bi9911839 CCC: $18.00
Published on Web 10/23/1999

Table 1: Affinity Measurements Reveal That Synthetic Filaments Resemble Authentic Tau Filaments with Respect to Monoclonal Antibody Alz50 Immunoreactivity

antibody[a]	htau40[b] K_d (nM)	PHF[b] K_d (nM)	synthetic polymer[c] K_d (nM)	ratio[d] htau40:PHF	ratio[d] htau40:SF
Tau-5	0.26 ± 0.01	0.35 ± 0.02	0.31 ± 0.08	0.74 ± 0.05	0.84 ± 0.22
Alz50	25.0 ± 3.8	$\leq 0.33 \pm 0.11$	1.82 ± 0.12	$\geq 76 \pm 28$	13.7 ± 2.3

[a] Tau-5 (*16*); Alz50 (*15*). [b] Data from ref *17*. [c] Prepared from recombinant htau40 and AA as described under Experimental Procedures. [d] Ratio = K_d of tau binding/K_d of PHF−tau binding. Values less than unity reflect selectivity for tau, whereas values greater than unity reflect selectivity for PHF−tau.

(Albert Einstein College of Medicine, New York, NY). AA was reconstituted in 100% ETOH and stored under argon gas at −80 °C.

Tau Polymerization Assay. Under standard conditions, htau40 (0.08−4 μM) was incubated with AA (10−100 μM) in buffer A (10 mM HEPES, pH 7.4, 100 mM NaCl) under reducing conditions (5 mM DTT) either at room temperature or at 37 °C. Samples were processed for fluorescence spectroscopy or electron microscopy as described below.

Electron Microscopy. Aliquots of tau polymerization reactions were removed as a function of time (0−7 days) and immediately treated with 2% glutaraldehyde (final concentration) at room temperature for ≥1 h. Samples were mounted on Formvar/carbon-coated 300 mesh grids, negatively stained with 2% uranyl acetate (*14*), and viewed in a JEOL JEM-1220 transmission electron microscope operated at 60 kV. Images were captured either digitally on a Kodak Megaplus 1.6i digital camera or on black and white film, and processed with Metamorph software (Universal Imaging Corp, West Chester, PA). Filament dimensions were quantified from six random images per grid. Filament lengths were calibrated using parallel images of 200 nm latex beads (Electron Microscopy Sciences, Fort Washington, PA). Total filament lengths (i.e., the sum total of all filament lengths within a field) are reported ± standard deviation.

Fluorescence Spectroscopy. The principles of this method have been described previously (*12*, *19*, *20*). ThS was added to tau polymerization reaction products at a final concentration of 0.5−5 μM. After gentle mixing, fluorescence was read directly in an SLM 8000c fluorimeter (λ_{ex} = 440 nm; λ_{em} = 490 nm; 1 nm bandwidth) operated at 800 V, gain 10, and slit 16 at room temperature. Under these conditions, polymer-bound ThS fluoresces brightly, whereas free ThS or ThS in the presence of monomeric tau or fatty acid does not (see below). For kinetic analysis, AA was added directly to a stirred cell containing htau40, buffer A, DTT, and ThS, and fluorescence data were collected every 2−4 s for up to 60 min.

Analytical Methods. Monoclonal antibody affinities and protein contents were estimated as described previously (*17*). All statistical errors are reported as standard deviations unless otherwise noted.

Tau polymerization time courses were fit as a two-phase exponential association reaction: $Y = Y_{max1}(1 - e^{-kob1 \cdot X}) + Y_{max2}(1 - e^{-kob2 \cdot X})$, where Y is proportional to the amount of tau polymer, X is time, and k_{ob} is the observed rate constant of the reaction. The time required for half-maximal signal development ($t_{1/2}$) was calculated ± 95% confidence intervals.

Reaction order was established from double-logarithmic (van't Hoff) plots as described previously (*21*). Results are reported as slope ± standard error of the estimate.

Scatchard analysis of htau40 polymerization reactions consisted of plotting ν/[x] vs ν, where ν is polymer-bound ThS fluorescence, and where [x] approximates the free concentration of varied ligand. All analyses assume validity of the steady-state assumption, and that $[x]_{free} \approx [x]_{total}$.

RESULTS

Synthetic Filaments Resemble Authentic Tau Filaments Immunologically. To assess the relationship between synthetic SFs prepared from recombinant htau40 (*14*) and authentic PHFs isolated from AD brain (*18*), samples of each were compared on the basis of three criteria. First, the binding affinity between selected monoclonal antibodies and tau filaments was quantified. Previously, we showed that monoclonal antibodies against tau fall into selectivity classes: one, exemplified by antibody Tau-5, binds continuous epitopes on tau irrespective of aggregation state; another, exemplified by antibody Alz50, binds the PHF−tau conformation selectively (*17*). The relative selectivity of these antibodies for purified, synthetic SFs prepared from pure htau40 was assessed. All Scatchard plots were linear, indicating that Tau-5 and Alz50 interact with tau via single, noncooperative binding sites (*17*). The binding constants (K_d) calculated from these plots (summarized in Table 1) show that monoclonal antibody Tau-5 bound monomeric htau40, synthetic SFs created from htau40, and authentic PHFs with similar affinity. These data are consistent with Tau-5 binding a continuous epitope that is accessible and presented nearly identically in monomeric and filamentous tau. In contrast, the conformation-selective monoclonal antibody Alz50 bound synthetic filaments with ≈14-fold higher affinity than monomeric htau40. Although this level of selectivity is not as great as that between authentic PHF and monomeric htau40, the data suggest that tau in synthetic SFs has a conformation approaching that found in authentic PHF.

Synthetic Tau SFs Resemble Authentic PHFs in Their Ability To Bind ThS. As a second criterion of similarity, the ability of synthetic filaments to interact with ThS was assessed. This fluorescent probe is used routinely to identify elements of the fibrillar pathology (neurofibrillary tangles, neuritic plaques, and neuropil threads) in Alzheimer's disease (AD) tissue. It is unusual in that both its excitation and its emission spectra shift to longer wavelengths upon binding tau filaments. These properties permit selective detection of filamentous tau in authentic fibrillar lesions of AD (Figure 1A). ThS also binds synthetic SFs formed from recombinant htau40 in vitro, yielding a red shift in excitation optimum, from 380 to ≈400 nm (Figure 1B), and a red shift in emission optimum from ≈445 (*19*) to ≈495 nm (Figure 1C). Similar Stokes shifts occur when ThS binds authentic PHF in vitro (*12*, *22*). These fluorescence changes appeared within

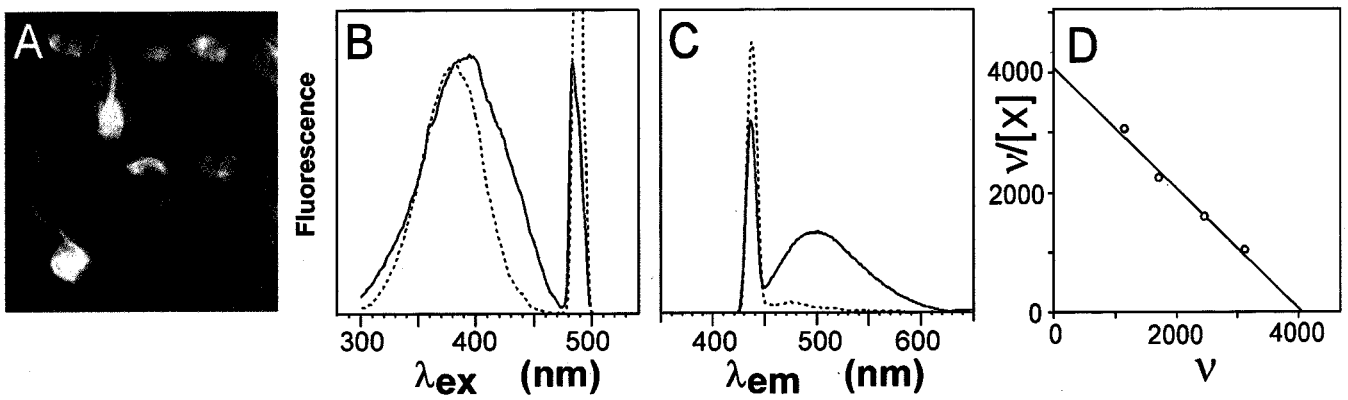

FIGURE 1: Synthetic filaments bind ThS. ThS is a fluorescent dye used to stain various pathological structures including NFT. (A) A 40 μm thick section of superior temporal gyrus from a late-stage case of AD stained with ≈200 μM ThS (10 min × 22 °C) and viewed under fluorescence microscopy (λ_{ex} band-pass filter = 400−440 nm; λ_{em} high-pass filter = 480 nm) reveals staining of tau filaments within authentic NFTs. (B, C) Fluorescence spectroscopy reveals that ThS also binds synthetic htau40 SFs. The optima for (B) excitation (estimated at fixed λ_{em} = 490 nm) and (C) emission (estimated at fixed λ_{ex} = 440 nm) of ThS fluorescence (2 μM) were determined in assembly buffer (10 mM HEPES, pH 7.4, 100 mM NaCl, 5 mM DTT) containing htau40 (2 μM) in the presence (solid line) or absence (dotted line) of AA (50 μM). Measurements were made after 1 h incubation at room temperature. AA-induced filament formation produces red Stokes shifts in both excitation (from ≈380 to ≈400 nm) and emission (from ≈445 to ≈495 nm) optima. Because of these Stokes shifts, the fluorescence of tau polymer-bound ThS can be detected with minimal interference from unbound ThS when λ_{ex} = 440 and λ_{em} = 490−510 nm. Neither htau40 nor AA alone induce shifts in ThS fluorescence. (D) Scatchard plot of ThS fluorescence (λ_{ex} = 440 nm; λ_{em} = 490 nm) measured after 1 h incubation under standard conditions at room temperature (1 μM htau40; 50 μM AA) in the presence of varying concentrations of ThS (0.5−2 μM), where ν is the fraction of bound ThS (approximated by dividing fluorescence by total ThS concentration) and [X] approximates free ThS concentration. These data are consistent with ThS interacting with synthetic htau40 SFs in a noncooperative manner through a single class of binding site.

seconds of mixing, and displayed classical saturation equilibria with respect to dye concentration. Scatchard plots of ThS binding to synthetic SFs were linear (estimated at λ_{ex} = 440 nm; λ_{em} = 490 nm), suggesting that ThS binds to a single class of sites on filaments and does not participate directly in the polymerization reaction. Binding proceeded with an apparent K_d of 0.96 ± 0.31 μM (Figure 1D). These data suggest that synthetic tau SFs retain the ThS pharmacophore found on authentic, AD-derived tau filaments and on synthetic PHF.

Synthetic Tau SFs Resemble Authentic Filaments Morphologically. As a final criterion of similarity, the packing of tau protomers within synthetic tau SFs and authentic PHFs was assessed through seeding experiments. When authentic PHFs were incubated (≤3 h) under standard conditions + AA in the absence of recombinant tau protein, they continued to appear in the transmission electron microscope as blunt-ended, short helical structures (Figure 2A). As shown previously (*14*), incubation (≤3 h) of htau40 under identical conditions yielded synthetic filaments of SF morphology (Figure 2B). Yet when htau40 was incubated under identical conditions in the presence of authentic PHFs, the latter were capable of serving as templates for the extension of synthetic filaments. When viewed at high magnification, the synthetic extensions appeared to have SF morphology, and typically grew from only one end of the PHF (Figure 2C). It should be noted that, under the solvent conditions and incubation times employed, no elongation of synthetic tau from authentic PHFs occurred in the absence of AA.

These synthetic PHF/SF chimeras resemble authentic chimeras isolated from AD brain (*5, 23*). The ability of PHFs to serve as templates for the elongation of synthetic SFs suggests that the tau−tau contacts and hence the internal packing of tau protomers are similar in synthetic SFs and authentic PHF. Furthermore, they suggest that PHFs are truly "paired", being composed of two intertwining SF-like hemifilaments. We conclude that the synthetic SFs we produce from recombinant htau40 are closely related to authentic PHFs in structure, and that they present a useful and relevant model for examining tau filament assembly.

Fatty Acid-Mediated Tau Filament Formation Proceeds via a Condensation Mechanism. Because the polymerization of recombinant htau40 is completely dependent upon the presence of polymerization inducers (*14*), it is possible to control and quantify the earliest events in tau filament formation. As shown in Figure 3, incubation of htau40 at low micromolar concentration under standard conditions did not yield filamentous material, even after 7 h of incubation (Figure 3A). In contrast, the addition of AA to physiological concentrations of htau40 (1−4 μM) resulted in the near-instantaneous formation of globular structures averaging 21.7 ± 6.7 nm (n = 187) in their longest dimension (Figure 3B). Within 1 h, nascent filaments up to 1 μm in length were visible (Figure 3C). Longer time points showed that filament elongation continued, but that the number of filaments or nucleation centers increased only slowly over time (Figure 3D). These results suggest that the primary role of tau polymerization inducers such as fatty acids is to nucleate the reaction (i.e., to facilitate the formation of small tau aggregates that serve as centers for elongation into filaments), and that the nucleation reaction is fast relative to filament elongation.

To extend this observation, the time course of tau polymerization was examined in real time using ThS fluorescence. As shown in Figure 1, and reported previously (*12, 20, 22*), the Stokes shift that occurs upon ThS binding to filaments allows selective detection of polymer in the presence of monomer. ThS fluorescence (λ_{ex} = 440 nm; λ_{em} = 490 nm) did not appear until fatty acid was added to htau40, again confirming that the reaction is fatty acid-dependent (Figure 4). Upon addition of AA, ThS fluorescence appeared immediately, and increased linearly for the

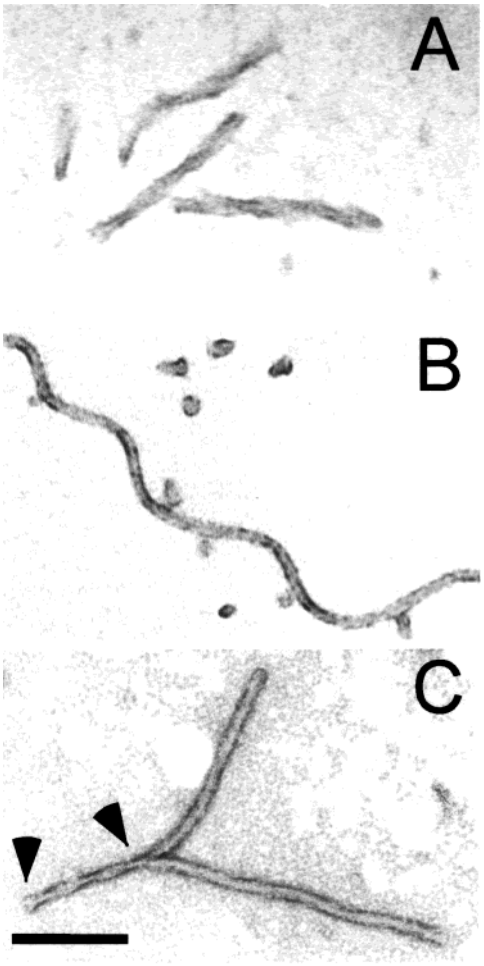

FIGURE 2: Synthetic tau filaments resemble authentic AD-derived filaments morphologically. The similarity between synthetic SFs prepared from recombinant htau40 and authentic AD-derived tau filaments is apparent when tau is polymerized onto PHF "seeds" and viewed in the transmission electron microscope. (A) Authentic PHFs incubated under standard assembly conditions (<3 h) in the absence of htau40 and AA remain as PHF. (B) Recombinant htau40 (4 μM) incubated in the presence of AA (100 μM) forms synthetic filaments with straight morphology. (C) Authentic PHFs incubated under standard assembly conditions in the presence of htau40 (4 μM) and AA (100 μM) over short (<3 h) time periods serve as seeds for elongation of synthetic htau40 SFs. The portion of a representative chimera corresponding to authentic PHF lies between arrowheads. The presence of authentic PHF/SF chimeras in AD brain has been noted previously (*5*, *23*). These data suggest that the PHF is truly "paired", being composed of two intertwining SF-like filaments. Furthermore, they suggest that the tau−tau contacts between tau monomers in synthetic SFs and authentic tau filaments are similar. Bar = 100 nm.

first 10 s of reaction. Thereafter, the extent of ThS fluorescence increased nonlinearly for the remainder of the time course. These data fit a two-phase exponential association (modeled as described under Experimental Procedures; $r^2 = 0.991$). When measured at physiological tau concentration (2 μM), the first phase had a $t_{1/2}$ of 22.5 ± 0.5 s, whereas a second, slower phase had a $t_{1/2}$ of 6.3 ± 0.2 min. Both phases correlated with the total length of tau filaments produced as estimated by quantitative electron microscopy (Figure 4). These data suggest that polymeric species of htau40 produced following exposure to AA, including small aggregates appearing at the earliest time points, are ThS-positive. The results also suggest that AA-dependent tau polymerization proceeds through a condensation mechanism, with rapid nucleation into small, ThS-positive structures followed by a slower elongation phase yielding SFs.

Tau Filament Nucleation Is Cooperative. Typically, polymerization reactions that proceed by a condensation mechanism exhibit a cooperative dependence on protomer concentration, and a threshold or "critical" concentration for assembly. To determine whether fatty acid-mediated htau40 assembly exhibited these properties, the relationship between htau40 concentration and ThS fluorescence (λ_{ex} = 440 nm; λ_{em} = 490 nm) appearing in 1 h was examined. The results show that the reaction is biphasic (Figure 5A). The first phase was observed at tau concentrations below 0.5 μM, and consisted of a graded increase in fluorescence as tau concentrations were raised. When plotted on double-logarithmic axes (van't Hoff plot), a slope of 0.74 ± 0.17 was obtained, indicating that the dependence of ThS fluorescence on tau concentration was essentially linear. This phase may correspond to conformational changes in tau monomers. The second phase spanned tau concentrations ranging from 0.6 to 1.2 μM, and consisted of a steep rise in fluorescence with increasing tau concentration. Within this range, fluorescence increased as the third power of tau concentration (van't Hoff slope = 3.00 ± 0.32 μM). On the basis of the abscissa intercept, the critical concentration (i.e., the minimal htau40 concentration required for self-association and polymerization in the presence of fatty acid) of tau polymerization was estimated as 0.50 ± 0.09 μM. This value lies well within the total concentration of all tau proteins thought to exist in normal neurons (see Discussion).

Fatty Acid Dependence of Tau Polymerization. To assess the dependence of tau assembly on fatty acid concentration, 2 μM htau40 was incubated with AA concentrations varying from 10 to 80 μM (Figure 5B). At low AA concentrations (10−30 μM), the reaction appeared graded but highly cooperative, with ThS fluorescence increasing as the third power of AA concentration (van't Hoff slope 2.89 ± 0.86; slope ± 95% confidence interval). The reaction then maximized (30−40 μM) and began decreasing (>40 μM). Similar biphasic behavior has been observed in other AA-dependent processes (*24*) and may reflect the critical micellization concentration (≈25 μM) of this fatty acid. Alternatively, it may result from sequestration of htau40 protomers at high AA concentration. These data demonstrate that tau polymerization is dependent on AA concentration, with filament formation requiring at least 10 μM AA.

Ligand-Dependent Tau Polymerization. Two limiting classes of ligand-dependent polymerizations have been characterized: a ligand-mediated reaction mechanism, wherein polymerization inducer must bind protomer before self-association; and a ligand-facilitated reaction mechanism, where inducer acts to stabilize preexisting aggregates of protomer. The two mechanisms can be distinguished experimentally by examining the ligand dependence of polymerization at varying protomer concentrations. For ligand-facilitated reactions, the potency of ligand increases with increasing concentrations of protomer (*25*). For ligand-mediated reactions, polymerization is protomer concentration independent. For cooperative systems, which yield nonlinear data plots, differences in ligand potency are most easily observed as changes in the ordinate intercept of Scatchard plots (*25*).

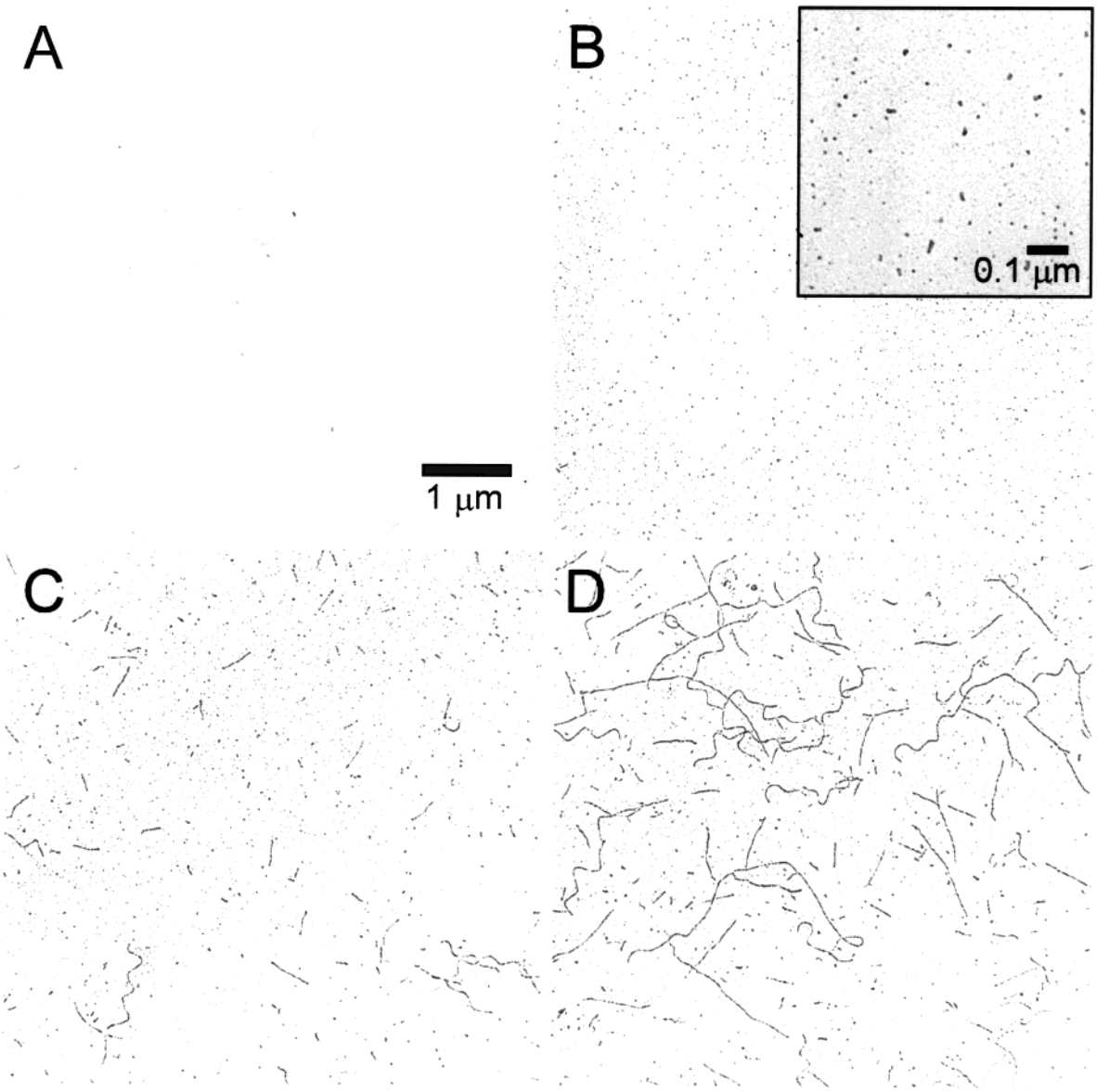

FIGURE 3: Fatty acid-induced tau filament formation is a rapid process. Recombinant htau40 (4 μM) was incubated in the absence (A) or presence (B−D) of AA (100 μM) under standard conditions. Aliquots were removed as a function of time (A, 7 h; B, 0 h; C, 1 h; D, 3 h) and processed for transmission electron microscopy as described under Experimental Procedures. (A) In the absence of AA, htau40 does not polymerize over 7 h of incubation. (B) The addition of AA to physiological concentrations of htau40 results in the immediate formation of globular structures averaging 21.7 ± 6.7 nm (n = 187) in their longest dimension (see inset for higher magnification). (C) Within 1 h of incubation, these extend to form nascent filaments up to 1 μm in length. (D) After 3 h of incubation, synthetic filaments with SF morphology continue to elongate, while the number of filaments increases only slowly. These results suggest that tau polymerization begins with the formation of nuclei immediately upon fatty acid addition and is followed by a slower elongation phase.

To distinguish which mechanism best describes AA-dependent htau40 polymerization, AA-dependent induction of ThS fluorescence (λ_{ex} = 440 nm; λ_{em} = 490 nm) was assessed at three different htau40 concentrations (at or above the critical concentration). Discontinuities appearing at higher AA concentrations were avoided by examining the reaction in detail only within the early, cooperative phase observed at low AA concentrations (10−30 μM). When these data were plotted in Eadie−Scatchard format (Figure 6), a hyperbolic plot reflecting positive cooperativity was observed (*26*). Plots of this shape are typical of self-associating systems that bind small-molecule ligands (*25*). As tau protomer concentration was varied, no changes in the potency of AA as polymerization inducer were detected. In each case, ThS fluorescence was first detectable at 10 μM AA. This is apparent as all three curves share the same ordinate intercept, which is proportional to the potency of AA and the number of potential AA binding sites on tau (Figure 6). Assuming the number of arachidonic acid binding sites does not vary with tau concentration, these data suggest that the AA dependence of tau polymerization is not dependent on protomer concentration, and that the reaction mechanism is most consistent with a ligand-mediated scheme (*25*). That is, under the conditions of these experiments, AA-induced tau filament formation follows an ordered reaction mechanism, with the binding of AA to tau preceding its homopolymerization. On the basis of the critical concentration data discussed above, the process can begin at htau40 concentrations as low as 0.5 μM, and is detectable at AA concentrations as low as 10 μM.

SFs Can Serve as Precursors to PHFs. Over the short time courses analyzed above, the morphology of htau40

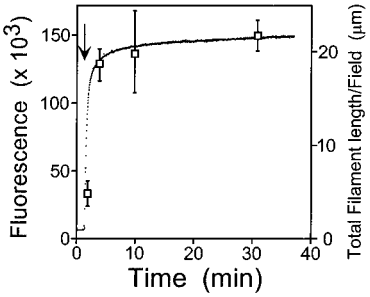

FIGURE 4: Short time course of tau filament formation. Recombinant htau40 (4 μM) was incubated under standard conditions for 30 min with constant stirring in the presence of ThS while fluorescence intensity (λ_{ex} = 440 nm; λ_{em} = 490 nm) was recorded every 2 s. After ≈3 min incubation, AA (75 μM final concentration) was added (arrow). The left ordinate records a rapid increase in ThS fluorescence upon addition of AA (dots). Aliquots from a parallel reaction were taken at t = 1, 3, 9, and 30 min, and analyzed by quantitative transmission electron microscopy as described under Experimental Procedures. Resultant estimates of total filament length/field are shown on the right ordinate (open squares), with error bars corresponding to ± one standard deviation. These data show a close kinetic correlation between total AA-induced total filament length as estimated by electron microscopy and the AA-induced increase in the intensity of ThS fluorescence.

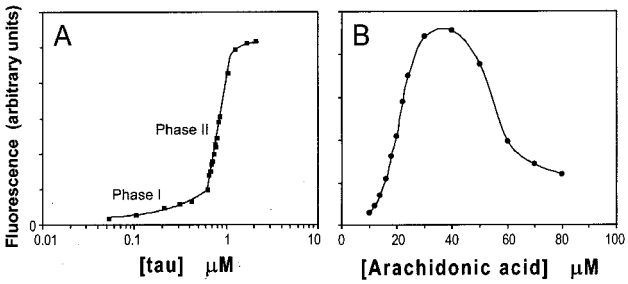

FIGURE 5: Tau filament formation is cooperative with respect to protomer and inducer concentrations. Tau polymerization was monitored by ThS fluorescence (λ_{ex} = 440 nm; λ_{em} = 490 nm) after 1 h of incubation under standard conditions at room temperature in the presence of variable concentrations of (A) htau40 (0.05−2 μM htau40; 50 μM AA) or (B) AA (10−80 μM AA; 2 μM htau40). See text for details.

polymers produced under reducing conditions is almost exclusively that of SFs (*8*, *14*). On the basis of monoclonal antibody affinity, ThS reactivity, and morphology, these filaments represent hemifilaments of the PHF. To ascertain the long-term fate of these filaments, aliquots of htau40 incubated with AA over a period of days at 37 °C were examined by transmission electron microscopy. The results, illustrated in Figure 7, reveal that htau40 can form filaments with extensive PHF-like morphology after 2 days of incubation. These results suggest that SFs can lead to PHFs through annealing of near-neighbors, or by serving as "seeds" for slow extension of a second hemifilament to form a full PHF.

DISCUSSION

Although a growing body of evidence suggests the polymerization of tau protein into the filamentous forms found in neurodegenerative disease is a guided process, the exact nature of the inducer active pathologically and its mechanism of action is contentious. In vitro data suggest that polyanions, such as heparin or RNA, can guide the formation of PHF−tau from recombinant tau protein, so long as the tau is modified by oxidation and covalent dimer

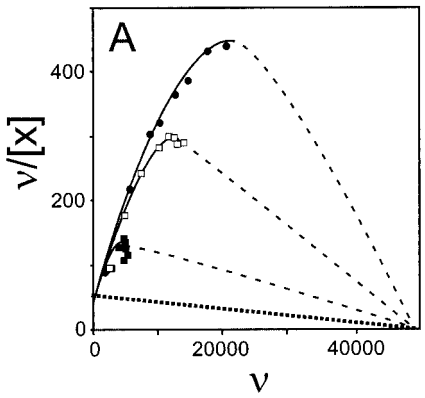

FIGURE 6: Fatty acid-induced tau filament formation proceeds via a ligand-dependent mechanism. Tau polymerization was monitored by ThS fluorescence (λ_{ex} = 440 nm; λ_{em} = 490 nm) after 1 h incubation under standard conditions at room temperature in the presence of variable concentrations of AA (10−30 μM). Results are depicted as Scatchard plots, where ν is polymer-bound ThS fluorescence and [X] approximates the concentration of free AA. Curves were generated at htau40 concentrations of 0.5 μM (■), 0.8 μM (□), and 1 μM (●) htau40. Dashed lines represent curves extrapolated above the critical micellization constant of AA, assuming that the total number of AA interaction sites (the abscissa intercept) does not vary with tau protomer concentration. The resultant plots are convex because of the cooperative relationship between AA concentration and tau filament formation (see Figure 5). A hypothetical plot of a noncooperative binding reaction is shown for comparison as a dotted line (see Figure 1D for an actual example). Each plot retains a common intercept on the ordinate, suggesting that the potency of AA as an inducer of htau40 polymerization does not depend on htau40 protomer concentration. This pattern is consistent with a ligand-mediated mechanism and inconsistent with a ligand-facilitated mechanism (*25*). In ligand-dependent processes, binding of ligand (AA) is an obligate first step in the polymerization reaction.

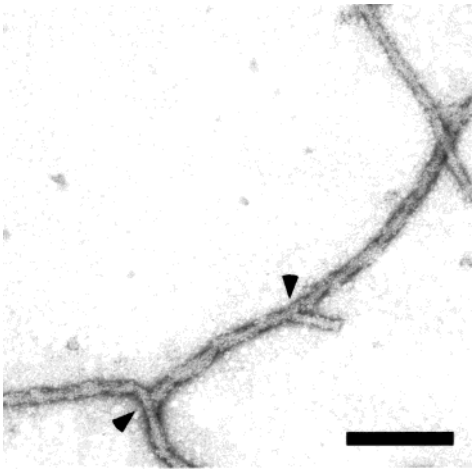

FIGURE 7: Fatty acid-induced filaments adopt PHF morphology when incubated for long periods. Recombinant htau40 (4 μM) was incubated (37 °C) with AA (100 μM) under standard conditions for 7 days, during which time aliquots were removed and subjected to transmission electron microscopy. After 2 days of incubation (shown above), extensive helical morphology became apparent (periodicity = 88 ± 15 nm; n = 16 periods). The presence of many junctions and spurs (arrowheads) suggests that SFs may evolve into PHFs by annealing with near-neighbors. Bar = 100 nm.

formation (*11*, *12*) or by selective proteolysis (*13*). Intact, full-length monomeric tau protein (htau40) assembles poorly under these conditions (*9*, *11*, *27*). Here we have shown that another class of polymerization inducer, AA, can promote tau filament formation much more efficiently than polyanions

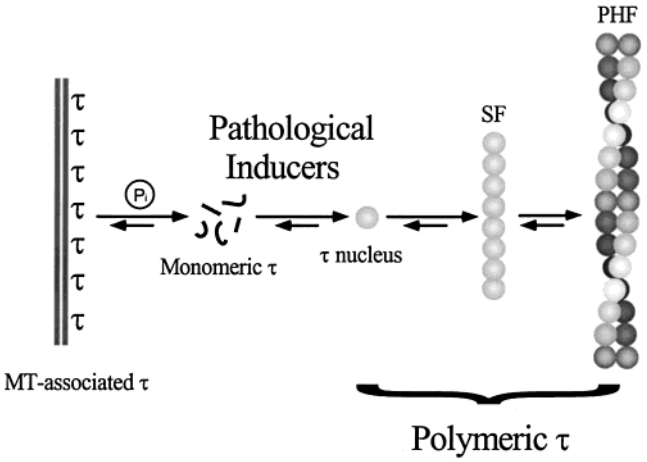

FIGURE 8: Hypothetical model of tau filament formation in neurodegenerative disease. See text for details.

under normal physiological conditions of pH, temperature, ionic strength, and tau protein concentration. Moreover, initiation of the reaction does not require phosphorylation or other modification of full-length tau protein, and proceeds under the reducing conditions encountered within normal eukaryotic cells (*28*).

These results support an alternative mechanism of tau filament assembly (Figure 8). Under basal conditions, total intracellular tau concentrations average ≈2 μM in brain (*29*). Tubulin is present in vast excess (≈20 μM dimer; *30*), and the K_d for tau/tubulin interaction is low (≈100 nM; *31*). Thus, in the absence of phosphorylation, it is predicted that >99% of total tau should be in complex with microtubules, leaving a free intracellular tau concentration far below the critical concentration required for tau homopolymerization. In reality, tau protein normally contains covalent phosphate which can increase the K_d for tau/tubulin interaction (*32*), and drive up the intraneuronal concentration of free tau. The first step in the process of filament formation may involve hyperphosphorylation, which can further drive monomeric tau concentrations to levels that support SF formation. On the basis of data presented here for htau40, the critical concentration for fatty acid-mediated filament formation is reached when 25% (≈0.5 μM) of total tau is free in solution. Still, elevated tau concentrations produced by phosphorylation or other mechanisms do not lead to filament formation directly. Rather, we propose that under reducing conditions the transient or prolonged elevation in inducer concentration results in very rapid nucleation of monomeric tau into nascent filaments. Nucleation follows a ligand-mediated mechanism: that is, binding events are strictly ordered, with inducer (AA) binding being an obligate first step. Binding may stabilize an altered conformation of tau, which then undergoes homopolymerization. Once nucleation has occurred, tau filaments elongate with straight morphology, corresponding to single hemifilaments of the PHF. But over extended time periods (days), the filaments can attain the classic dimensions of the PHF. The evolution of PHF from SF observed in vitro may result from annealing and joining of neighboring SFs, or from slow extension of a second hemifilament to form a full PHF. The latter process may involve oxidation, for although the Cys residues found within the microtubule repeat domain remain fully reduced for 24 h under the DTT concentrations used here (*33*), they may slowly oxidize to form tau dimers after this time. Whatever the mechanism, an apparent progression of authentic tau filaments from SF to PHF morphology has been observed in AD brain (*7*). In other tau filament-forming diseases, such as progressive supranuclear palsy, SFs actually predominate (*34, 35*).

As noted above, tau polymerization can be promoted by substances other than fatty acids, such as polyanions. Yet in addition to being inefficient, and requiring oxidation or truncation of tau protein to proceed, these substances are poorly placed to act in vivo. For example, heparin is primarily extracellular, whereas tau protein is exclusively intracellular. RNA is intracellular, and present at high concentration, but is complexed with protein rather than existing free in solution. In contrast, several lines of evidence suggest that anionic lipids or lipid-derived substances (such as fatty acids) may play a role in neurodegenerative disease. First, ultrastructural analysis of AD brain biopsy material reveals that tau filaments appear to begin or end in association with cellular membranes (*36*). The clear implication is that an essential component of the assembly machinery is membranous. Although this material could be a protein or other matter, the ability of fatty acids and polyanions to promote tau polymerization strongly suggests it is the lipid component of the membrane itself that seeds, nucleates, or somehow facilitates tau assembly. Second, tau protein binds lipid (*37, 38*), NFTs label with antiganglioside antibodies (*39*), and isolated PHFs contain glycolipid (*40, 41*). Indeed, a pool of tau associates with the plasma membrane in situ (*42*). Thus, tau−membrane interaction may be a facet of normal tau function that is perturbed in AD. Finally, genetic studies reveal that a risk factor for AD is apolipoprotein E (apoE), a lipid carrier molecule (*43*). ApoE could affect tau polymerization indirectly by influencing the lipid composition of cellular membranes. Again, although the work presented herein relies exclusively on AA, it is possible that tau polymerization is mediated in vivo by other lipids, or by AA derivatives produced by enzymatic (e.g., prostaglandins) or nonenzymatic means (e.g., isoprostanes; *44*). Indeed, inhibition of prostaglandin-mediated tau polymerization may contribute to the ameliorative effects observed on treatment of AD cases with cyclooxygenase inhibitors (*45*).

The model presented above has important mechanistic implications for the formation of fibrillar pathology in vivo. First, we have shown that filament nucleation proceeds rapidly in the absence of tau phosphorylation, a result consistent with the role of "hyperphosphorylation" in filament assembly being indirect. It cannot be excluded, however, that phosphorylation at appropriate sites alters the critical concentration of tau assembly, or affects the rates of nucleation or elongation. Second, we predict that tau filaments can be nucleated in response to short-term insults that result in transient phosphorylation and elevation of polymerization inducers such as fatty acids. The stability of the resultant tau filaments may exceed the lifetime of the insult. This suggests a potential link between environmental factors (e.g., blows suffered by a prize fighter) and the onset of neurofibrillary changes associated with neurodegenerative disease (e.g, *dementia pugilistica*). It also suggests a mechanism by which changes in tau conformation can accumulate with time. This is in marked contrast to the proposed oxidative pathway of PHF formation, which by having a critical concentration of 1 μM dimer, requires that essentially

all brain tau be free and dimerized before polymerization can occur (*13*).

The model also has implications for tau filament structure. Despite being disordered in solution (*22*), tau monomers pack into filaments displaying organized morphology. The conformational changes in tau protomers that accompany filament formation can be sensed by conformation-selective monoclonal antibodies such as Alz50 (*17*). In fact, tau filaments present a novel pharmacophore that can be bound and detected with small-molecule probes such as ThS. The data presented here confirm that SFs and PHFs are closely related structurally (*5*). Indeed, the PHF is truly "paired", consisting of two SF-like hemifilaments wound around each other, rather than being a twisted ribbon (*46*) or a disordered aggregate (*47*). Furthermore, seeding experiments with authentic PHFs suggest that filaments maintain directionality in their elongation, with growth occurring more efficiently from one end (the "+" end) than the other end (the "−" end). Similar behavior (nucleation dependence and polarity of assembly) has been observed for polymers of actin and tubulin (*48*). The ability of PHFs to seed formation of SF "forks" primarily off one end is consistent with its hemifilaments being aligned in a parallel fashion. Because tau dimers are aligned in an antiparallel arrangement (*49, 50*), this suggests that the axis of filament elongation is perpendicular to the axis of dimer formation (*51*).

In summary, we have established the mechanism of assembly for htau40 under reducing conditions. The data provide a base line for comparison with other tau isoforms (*52*), which may differ in their ability to nucleate and extend filaments. Indeed, familial forms of Frontal Lobar Atrophy contain mutations in the tau gene, one of which acts to alter the balance of tau isoforms expressed (*53, 54*). It will be important to assess the assembly properties of each of the six known human tau isoforms under these conditions.

ACKNOWLEDGMENT

We thank Nupur Ghoshal (Northwestern University Medical School, Chicago, IL) for samples of ThS-stained neocortex, and Drs. Hana Ksiezak-Reding and Peter Davies (Albert Einstein College of Medicine, Bronx, NY) for gifts of PHF tau and monoclonal antibody Alz50, respectively.

REFERENCES

1. Goedert, M. (1993) *Trends Neurosci. 16,* 460−465.
2. Wisniewski, K., Jervis, G. A., Moretz, R. C., and Wisniewski, H. (1979) *Ann. Neurol. 5,* 288−294.
3. Braak, E., Braak, H., and Mandlkow, E.-M. (1994) *Acta Neuropathol. 87,* 554−567.
4. Feany, M. B., and Dickson, D. W. (1996) *Ann. Neurol. 40,* 139−148.
5. Crowther, R. A. (1991) *Proc. Natl. Acad. Sci. U.S.A. 88,* 2288−2292.
6. Perry, G., Mulvihill, P., Manetto, V., Autilio-Gambetti, L., and Gambetti, P. (1987) *J. Neurosci. 7,* 3736−3738.
7. Perry, G., Kawai, M., Tabaton, M., Onorato, M., Mulvihill, P., Richey, P., Morandi, A., Connolly, J. A., and Gambetti, P. (1991) *J. Neurosci. 11,* 1748−1755.
8. Wilson, D. M., and Binder, L. I. (1995) *J. Biol. Chem. 270,* 24306−24314.
9. Pérez, M., Valpuesta, J. M., Medina, M., Montejo de Garcini, E., and Avila, J. (1996) *J. Neurochem. 67,* 1183−1190.
10. Goedert, M., Jakes, R., Spillantini, M., Hasegawa, M., Smith, M., and Crowther, R. A. (1996) *Nature 383,* 550−553.
11. Kampers, T., Friedhoff, P., Biernat, J., Mandelkow, E., and Mandelkow, E. (1996) *FEBS Lett. 399,* 344−349.
12. Friedhoff, P., Schneider, A., Mandelkow, E.-M., and Mandelkow, E. (1998) *Biochemistry 37,* 10223−10230.
13. Friedhoff, P., von Bergen, M., Mandelkow, E.-M., Davies, P., and Mandelkow, E. (1998) *Proc. Natl. Acad. Sci. U.S.A. 95,* 15712−15717.
14. Wilson, D. M., and Binder, L. I. (1997) *Am. J. Pathol. 150,* 2181−2195.
15. Wolozin, B. L., Pruchnicki, A., Dickson, D. W., and Davies, P. (1986) *Science 232,* 648−650.
16. LoPresti, P., Szuchet, S., Papasozomenos, S. C., Zinkowski, R. P., and Binder, L. I. (1995) *Proc. Natl. Acad. Sci. U.S.A. 92,* 10369−10373.
17. Carmel, G., Mager, E. M., Binder, L. I., and Kuret, J. (1996) *J. Biol. Chem. 271,* 32789−32795.
18. Ksiezak-Reding, H., and Wall, J. S. (1994) *Neurobiol. Aging 15,* 11−19.
19. Naiki, H., Higuchi, K., Hosokawa, M., and Takeda, T. (1989) *Anal. Biochem. 177,* 244−249.
20. LeVine, H. (1993) *Protein Sci. 2,* 404−410.
21. Kuret, J., and Schulman, H. (1985) *J. Biol. Chem. 260,* 6427−6433.
22. Schweers, O., Schonbrunn-Hanebeck, E., Marx, A., and Mandelkow, E. (1995) *J. Biol. Chem. 269,* 24290−24297.
23. Wischik, C. M., Crowther, R. A., Stewart, M., and Roth, M. (1985) *J. Cell Biol. 100,* 1905−1912.
24. Hwang, S. C., Jhon, D.-Y., Bae, Y. S., Kim, J. H., and Rhee, S. G. (1996) *J. Biol. Chem. 271,* 18342−18349.
25. Cann, J. R. (1978) *Methods Enzymol. 48,* 299−307.
26. Dahlquist, F. W. (1978) *Methods Enzymol. 48,* 270−299.
27. Hasegawa, M., Crowther, A., Jakes, R., and Goedert, M. (1997) *J. Biol. Chem. 272,* 33118−33124.
28. Sen, C. K. (1998) *Biochem. Pharmacol. 55,* 1747−1758.
29. Alonso, A. C., Grundke-Iqbal, I., and Iqbal, K. (1996) *Nat. Med. 2,* 783−787.
30. Hiller, G., and Weber, K. (1978) *Cell 14,* 795−804.
31. Goode, B. L., Denis, P. E., Panda, D., Radeke, M. J., Miller, H. P., Wilson, L., and Feinstein, S. C. (1997) *Mol. Biol.Cell 8,* 353−365.
32. Biernat, J., Gustke, N., Drewes, G., Mandlekow, E., and Mandlekow, E. (1993) *Neuron 11,* 153−163.
33. DeTure, M. A., Zhang, E. Y., Bubb, M. R., and Purich, D. L. (1996) *J. Biol. Chem. 271,* 32702−32706.
34. Tellez-Nagel, I., and Wisniewski, H. M. (1973) *Arch. Neurol. 29,* 324−327.
35. Bugiani, O., Mancardi, G. L., Brusa, A., and Ederli, A. (1979) *Acta Neuropathol. 45,* 147−152.
36. Gray, E. G., Paula-Barbosa, M., and Roher A. (1987) *Neuropathol. Appl. Neurobiol. 13,* 91−110.
37. Yamauchi, P. S., and Purich, D. L. (1987) *J. Biol. Chem. 262,* 3369−3375.
38. Surridge, C. D., and Burns, R. G. (1994) *Biochemistry 33,* 8051−8057.
39. Emory, C. R., Ala, T. A., and Frey, W. H. (1987) *Neurology 37,* 768−772.
40. Sparkman, D. R., Goux, W. J., Jones, C. M., White, C. L., III, and Hill, S. J. (1991) *Biochem. Biophys. Res. Commun. 181,* 771−779.
41. Goux, W. J., Rodriguez, S., and Sparkman, D. R. (1995) *FEBS Lett. 366,* 81−85.
42. Brandt, R., Leger, J., and Lee, G. (1995) *J. Cell Biol. 131,* 1327−1340.
43. Corder, E. H., Saunders, A. M., Strittmater, W. J., Schmechel, D. E., Gaskell, P. C., Small, G. W., Roses, A. D., Haines, J. L., and Pericak-Vance, M. A. (1993) *Science 261,* 921−923.
44. Roberts, L. J., Montine, T. J., Markesbery, W. R., Tappr, A. R., Hardy, P., Chemtob, S., Dettbarn, W. D., and Morrow, J. D. (1998) *J. Biol. Chem. 273,* 13605−13612.
45. McGeer, E. G., and McGeer, P. L. (1998) *Exp. Gerontol. 33,* 371−378.
46. Pollanen, M. S., Markiewicz, P., Bergeron, C., and Goh, M. C. (1994) *Am. J. Pathol. 144,* 869−873.

47. Ruben, G. C., Novak, M., Edwards, P. C., and Iqbal, K. (1995) *Brain Res. 675,* 1−12.
48. Frieden, C. (1985) *Annu. Rev. Biophys. Chem. 14,* 189−210.
49. Wille, H., Drewes, G., Biernat, J., Mandelkow, E. M., and Mandelkow, E. (1992) *J. Cell Biol. 118,* 573−584.
50. Ksiezak-Reding, H., and Yen, S.-H. (1991) *Neuron 6,* 717−728.
51. Murthy, S. N. P., Wilson, J., Lukas, T. J., Kuret, J., and Lorand, L. (1998) *J. Neurochem. 71,* 2607−2614.
52. Goedert, M., Spillantini, M., Jakes, R., Rutherford, D., and Crowther, R. (1989) *Neuron 3,* 519−526.
53. Hutton, M., Lendon, C. L., Rizzu, P., Baker, M., Froelich, et al. (1998) *Nature 393,* 702−705.
54. Spillantini, M. G., Murrell, J. R., Goedert, M., Farlow, M. R., Klub, A., and Ghetti, B. (1998) *Proc. Natl. Acad. Sci. U.S.A. 95,* 7737−7741.

BI9911839